

## Article

# Random Raman Lasing in Diode-Pumped Multi-Mode Graded-Index Fiber with Femtosecond Laser-Inscribed Random Refractive Index Structures of Various Shapes

Alexey G. Kuznetsov <sup>1</sup>, Zhibzema E. Munkueva <sup>1</sup>, Alexandr V. Dostovalov <sup>1,2</sup>, Alexey Y. Kokhanovskiy <sup>3</sup> , Polina A. Elizarova <sup>1,2</sup>, Ilya N. Nemov <sup>1</sup>, Alexandr A. Revyakin <sup>1,2</sup>, Denis S. Kharenko <sup>1,2</sup> and Sergey A. Babin <sup>1,2,\*</sup> 

<sup>1</sup> Institute of Automation and Electrometry, 1 Ac. Koptuyug Ave., Novosibirsk 630090, Russia

<sup>2</sup> Physics Department, Novosibirsk State University, 2 Pirogov Str., Novosibirsk 630090, Russia

<sup>3</sup> Physics Department, ITMO University, 9 Lomonosov St., St. Petersburg 191002, Russia

\* Correspondence: babin@iae.nsk.su

**Abstract:** Diode-pumped multi-mode graded-index (GRIN) fiber Raman lasers provide prominent brightness enhancement both in linear and half-open cavities with random distributed feedback via natural Rayleigh backscattering. Femtosecond laser-inscribed random refractive index structures allow for the sufficient reduction in the Raman threshold by means of Rayleigh backscattering signal enhancement by +50 + 66 dB relative to the intrinsic fiber level. At the same time, they offer an opportunity to generate Stokes beams with a shape close to fundamental transverse mode (LP<sub>01</sub>), as well as to select higher-order modes such as LP<sub>11</sub> with a near-1D longitudinal random structure shifted off the fiber axis. Further development of the inscription technology includes the fabrication of 3D ring-shaped random structures using a spatial light modulator (SLM) in a 100/140 μm GRIN multi-mode fiber. This allows for the generation of a multi-mode diode-pumped GRIN fiber random Raman laser at 976 nm with a ring-shaped output beam at a relatively low pumping threshold (~160 W), demonstrated for the first time to our knowledge.

**Keywords:** fs laser inscription; random structures; Rayleigh backscattering; spatial light modulator; Raman laser; graded-index fiber; multi-mode; LD pumping; beam shape



**Citation:** Kuznetsov, A.G.; Munkueva, Z.E.; Dostovalov, A.V.; Kokhanovskiy, A.Y.; Elizarova, P.A.; Nemov, I.N.; Revyakin, A.A.; Kharenko, D.S.; Babin, S.A. Random Raman Lasing in Diode-Pumped Multi-Mode Graded-Index Fiber with Femtosecond Laser-Inscribed Random Refractive Index Structures of Various Shapes. *Photonics* **2024**, *11*, 981. <https://doi.org/10.3390/photonics11100981>

Received: 14 September 2024

Revised: 14 October 2024

Accepted: 15 October 2024

Published: 18 October 2024



**Copyright:** © 2024 by the authors. Licensee MDPI, Basel, Switzerland. This article is an open access article distributed under the terms and conditions of the Creative Commons Attribution (CC BY) license (<https://creativecommons.org/licenses/by/4.0/>).

## 1. Introduction

In early times of fiber optics, multi-mode fibers were treated as a less stable and more complicated media than single-mode fibers, which are able to guide fundamental transverse modes over huge distances without any distortions, even in the presence of nonlinear effects. Interest in multi-mode fibers has greatly increased in the last decade, thanks to new perspectives on their use for optical communications [1] and high-power lasers [2]. In addition to limited transmission capacity, their use is also justified by clear limitations in single-mode laser regimes either in active fibers (mainly photo-darkening and transverse-mode instability) or in passive fibers with Raman gain (mainly a necessity to use single-mode pumping); see [3] for more details.

Recently, Raman fiber lasers (RFLs) based on multi-mode graded-index (GRIN) fibers have attracted great interest because they may be directly pumped by laser diodes; see [4,5] for a review. Impressive results have already been achieved in generating relatively high power radiation at short wavelengths (<1 μm) not previously available, neither in active fibers doped with rare earth elements [3] nor in conventional RFLs based on single-mode passive fibers [6]. An attractive feature of such lasers is the efficient conversion of highly multi-mode pump radiation into the generated Stokes beam, the quality of which turns out to be much higher than that of the original pump beam, thanks to the Raman beam cleanup effect in GRIN fibers [7], leading to higher Raman gain for lower-order modes. The use in laser cavities of a fiber Bragg grating (FBG) inscribed by femtosecond (fs) pulses in

the cross-section of a GRIN fiber core, corresponding to the fundamental mode, makes it possible to further enhance the effect of beam cleaning for the generated Stokes radiation [4]. So, in a linear resonator consisting of an FBG pair, the generation of a Stokes beam at a wavelength of 976 nm with power of more than 50 W and beam quality of  $M^2 \approx 2$  during pumping by multi-mode laser diodes (LDs) with low beam quality ( $M^2 \approx 34$ ) at 940 nm has been obtained [8]. This scheme of pump-to-Stokes beam conversion demonstrates record brightness enhancement,  $BE \approx 73$ , for such types of lasers. In [9,10], a two-stage cascaded Raman laser has been demonstrated, and the characteristics of the output radiation in the schemes with two pairs of FBGs and with a half-open cavity for the second stage based on random Rayleigh backscattering in GRIN fiber itself instead of output fs-FBG were compared. It was shown that in the case of Rayleigh-based random lasing, the efficiency of pump conversion and the quality of the output second-order Stokes beam were higher. The use of random Rayleigh feedback at the second stage of the cascaded cavity appeared to be possible due to the fact that the quality of the first Stokes beam generated in the FBG cavity was quite high ( $M^2 \approx 2$ ). Therefore, the second Stokes threshold was relatively easy to achieve at relatively weak Rayleigh backscattering on natural refractive index fluctuations in a 1 km long GRIN fiber. For a random generation of the first Stokes wave in a half-open cavity with low-quality pumping, a much longer GRIN fiber [11] or much higher pump power [12] is required. So, more than 300 W of power for random lasing at the first Stokes wavelength of 1120 nm was obtained in a 62.5  $\mu\text{m}$  core GRIN fiber with  $\sim 700$  W multi-mode pumping by combined Yb-doped fiber lasers at 1070 nm [12]; however, the threshold pump power for such a random Raman laser was as high as  $\sim 500$  W.

It should be noted that natural Rayleigh backscattering (RBS) on frozen refractive index inhomogeneities inside a silica-based fiber core is widely used in laser applications [13]. However, the low backscattering coefficient ( $\alpha \sim 4.5 \times 10^{-2} \text{ km}^{-1}$ ) of a standard telecommunication fiber limits laser system performance and requires the use of an extended fiber length (1–10 s km) and high pump power in the case of a Raman fiber laser with random distributed feedback on intrinsic Rayleigh backscattering both in single-mode and multi-mode fibers. Therefore, artificially increasing the density of inhomogeneities allows for the enhancement of the backscattering level and random distributed feedback as a result, which offers new opportunities to develop random fiber lasers with improved performance [14], as well as more sensitive distributed sensing systems based on Rayleigh backscattering [15]. Among methods used to create artificial scattering structures [14–16], the fs laser-based technique is assumed to be the most promising and flexible for modification inside transparent materials such as silica fibers. Due to the nonlinear absorption of fs pulses in the near-IR range, the refractive index can be locally changed (inside the focal volume) with high spatial resolution, which allows for the creation of 1D-3D structures inside multi-mode non-photosensitive fibers through a polymer fiber coating by the point-by-point (P-b-P) writing technique [14]. With this method, it is possible to select specific regimes of refractive index modification depending on fs pulse energy and duration, in order to achieve the desired level of RBS enhancement and inserted optical losses. Additionally, fs laser inscription provides extremely high temperature stability (up to 1000 °C) of the induced refractive index changes [17].

As a rule, the direct P-b-P fs writing technique is based on the fiber translation relative to a static focal spot of the laser beam using high-precision linear positioning stages [14]. At the same time, the implementation of adaptive optics provides new opportunities for the direct P-b-P writing technique [18]. Recently, spatial light modulators (SLMs) have been shown to allow for scanning of a focal spot inside a static fiber using the phase modulation of a fs laser beam and thus writing periodic structures with desired refractive index profile along the fiber core [19]. In multi-mode fibers, the inscription of artificial Rayleigh reflectors by the conventional P-b-P writing technique in the near-axis area of the multi-mode core is shown to provide random Raman lasing with a relatively low threshold and predominant content of fundamental mode ( $LP_{01}$ ) in the output beam [14]. Meanwhile,

the new SLM-based technique is able to form more complicated structures, thus enabling more complete control of the mode composition of the generated output beam.

Here, we study an opportunity to obtain random Raman lasing in a multi-mode diode-pumped GRIN fiber Raman laser by means of enhanced backscattering in artificial fs-inscribed random structures used as an output reflector, both for fundamental and higher-order modes. We test random reflectors formed by the conventional P-b-P fs writing technique with different positions in the fiber core and demonstrate predominant generation in either fundamental ( $LP_{01}$ ) or next-order ( $LP_{11}$ ) transverse mode in the half-open GRIN fiber cavity with random distributed feedback provided by an artificial Rayleigh reflector. We also present opportunities for the new SLM-assisted writing technique of random structures providing higher-order mode selection. The inscription of ring-shaped random structures in multi-mode GRIN fiber with Rayleigh backscattering level enhancement of up to +66 dB/mm is demonstrated. The performed line-by-line (L-b-L) inscription of reflective structures with random distances along the fiber is optimized in terms of fs pulse energy, SLM frame rate, the overall length and average distances between the structures. The generation of a Raman fiber laser with a ring-shaped output laser beam at a relatively low threshold based on ring-shaped random structures inscribed in GRIN multi-mode fiber is demonstrated for the first time, to our knowledge.

## 2. Materials and Methods

With the use of an fs laser, we fabricated different types of artificial random reflectors inscribed by a focused fs laser beam inside the core of multi-mode GRIN fiber with 100/140  $\mu\text{m}$  core/cladding diameters (Figure 1).

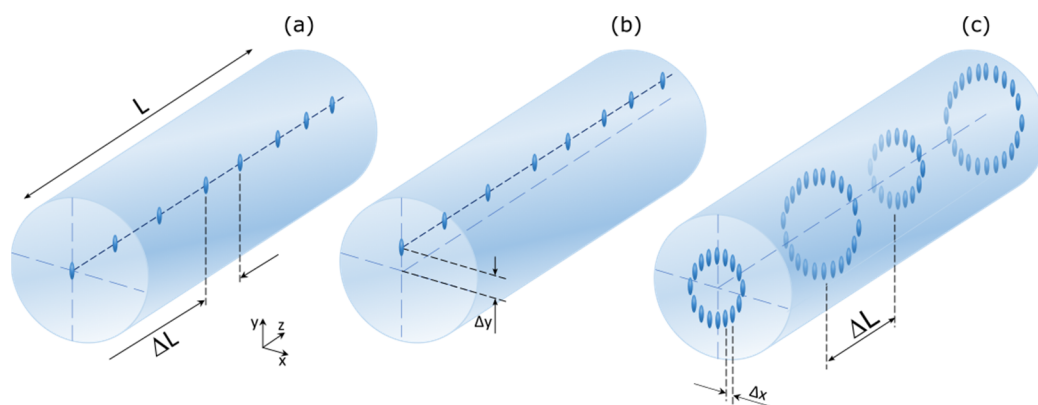


**Figure 1.** Artificial random reflectors of different types fs-inscribed inside the GRIN fiber core: (a) 1D in-line point reflector written along the fiber axis by the direct P-b-P technique, (b) similar 1D in-line reflector shifted off the axis; (c) 3D ring reflector written by SLM-assisted L-b-L technique, meaning that circular lines of overlapping points are inscribed in different planes with the average distance between the planes  $\Delta L$  and integral length of the structure  $L$ .

At, first, using the direct P-b-P fs writing technique, we inscribed an in-line (1D) random structure of point scatterers with variable integral length  $L$  and random distance between scattering points with average value  $\Delta L$ , directly focusing the fs laser beam on the fiber axis and translating the fiber along  $z$  axis (Figure 1a); see also [14] for details. Such a structure has been shown to provide a predominant reflection of the fundamental mode ( $LP_{01}$ ) with increased backscattering by about +50 dB/mm [14]; it was used as a reference for further steps towards the selection of higher-order transverse modes of the multi-mode GRIN fiber. As a next step, a similar 1D in-line random structure of point scatterers was fs-inscribed by the P-b-P writing technique, but with a transverse shift  $\Delta y$  off the fiber axis for the sake of predominant selection of the next transverse mode ( $LP_{11}$ ); see Figure 1b.

To test the opportunity of fabricating random structures with arbitrary 3D shapes for the selection of higher-order modes in a GRIN fiber, we applied the SLM-assisted

fs writing technique [19] with corresponding modifications aiming to achieve increased backscattering level enhancement with lower losses inserted. In this case, the phase of the Gaussian beam from a femtosecond laser, Pharos-6W by Light Conversion (Vilnius, Lithuania), with maximum pulse energy of >3 μJ at 1026 nm and a pulse duration of ~230 fs was modulated by the reflective phase-only SLM Holoeye Pluto-2.1-NIR-149 by HOLOEYE Photonics AG (Berlin, Germany) for the movement of the focal spot within the static fiber core (Figure 2). The ring structures inside the multi-mode fiber core were inscribed in randomly spaced cross-sections of the fiber core with an average longitudinal distance ΔL (see Figure 1c) by setting the pre-calculated phase masks according to the following expressions:

$$\begin{aligned} \varphi(x, y) &= \varphi_{grating} + \varphi_{tilt} \\ \varphi_{tilt}(x, y) &= k_x x + k_y y, \end{aligned}$$

where  $\varphi_{grating}(x, y) = (2\pi/\Lambda) \times y$  is the phase mask representing periodic grating to obtain a first-diffraction-order beam;  $\varphi_{tilt}(x, y)$  is the phase mask for movement of the focal spot inside the objective field of view ( $x_f, y_f$ ) along and perpendicular to the fiber axis, correspondingly;  $x, y$  are the coordinates relative to the center of the SLM screen;  $k_x, k_y$  are parameters depending on the tilt angle of the beam with coordinates  $x_f, y_f$  in the focal plane of objective with focal distance  $f$  as follows:

$$\frac{\lambda k_x}{2\pi} = \frac{x_f}{\sqrt{f^2 + x_f^2}},$$

where  $\lambda$  is the laser wavelength. In the approximation of  $x_f \ll f$ , we can rewrite  $\varphi_{tilt}$  in the following way:

$$\varphi_{tilt} = \frac{2\pi x_f}{\lambda f} x + \frac{2\pi y_f}{\lambda f} y.$$

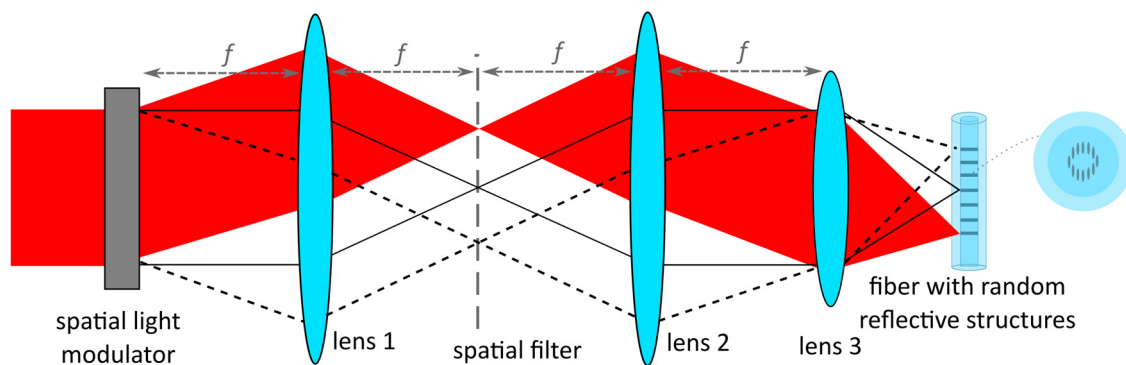


**Figure 2.** Optical scheme for SLM-assisted writing of random reflective structures using a 4f system with a focus length of 20 cm.

For a displacement of the focal spot in the depth along the  $z$  axis (focusing or defocusing depending on the sign of  $z_f$ ), the following phase mask was generated:

$$\begin{aligned} \varphi(x, y) &= \varphi_{grating} + \varphi_{focus} \\ \varphi_{focus} &= \frac{\pi z_f}{\lambda f^2} (x^2 + y^2), \end{aligned}$$

where  $z_f$  is the depth displacement from the initial focal plane at the condition of  $z_f \ll f$ .

To write ring structures, the  $z$  coordinate was set to the following value:  $z_f = \frac{\sqrt{R^2 - y_f^2}}{n}$ , where  $R$  is the ring radius and  $n$  is the refractive index of the fiber core.

After SLM (see Figure 2), the fs laser beam passed through the 4f system with a focus length of 20 cm, which made it possible to separate the diffraction orders in space in the Fourier plane, where a spatial filter was located for selection and inscription in +1 order. Furthermore, the laser beam was focused by the objective Mitutoyo APO NIR 20× by Mitutoyo Europe GmbH (Neuss, Germany) into the fiber core located on the 3D stage PlanarDL-100XY-PL4 by Aerotech GmbH (Fürth, Germany).

Before writing Rayleigh reflectors with complex geometries, we optimized inscription parameters (fs pulse energy, SLM frame rate, the overall length and distances of random structures along the fiber), which allowed us to achieve maximum Rayleigh backscattering enhancement with minimal inserted optical losses. For this purpose, we inscribed Rayleigh reflective structures with random distances along the fiber using the line-by-line method in single-mode fiber. It was observed that an increase in fs pulse energy leads to a larger inhomogeneity size and, consequently, a higher backscattering signal. The SLM frame rate determines the energy efficiency of the laser beam reflected from the SLM. The overall length and random distance along the fiber between random structures define the concentration of scattering inhomogeneities, which influences both the Rayleigh backscattering and inserted loss level. As a result, optimal inscription parameters (pulse energy of about 3  $\mu$ J, SLM frame rate of 5 Hz, the overall length and average distance between structures along the fiber of 2 mm and 5  $\mu$ m, respectively) were found.

Further, ring-shaped random structures were inscribed in a 100/140  $\mu$ m GRIN multi-mode fiber using the optimal inscription parameters found, which allowed us to achieve Rayleigh backscattering enhancement of up to +66 dB/mm above the natural RBS level (Figure 3a) at the integral loss level comparable to those for 1D structures described above. The average value and random variation of the distance between rings and the diameter of ring structures were within  $5 \pm 0.5$   $\mu$ m and  $20 \pm 10$   $\mu$ m ranges, respectively, which allowed us to obtain a broadband reflection spectrum with an integral reflection coefficient of  $\sim 0.01\%$  (Figure 3b).

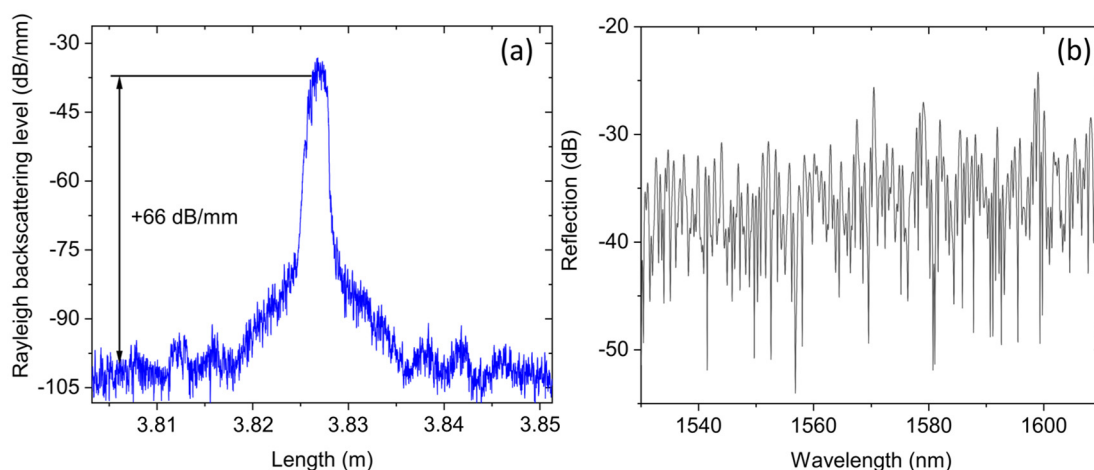


**Figure 3.** Rayleigh backscattering level (a) and reflection spectrum (b) of ring-shaped random structure with length  $L = 2$  mm inscribed in GRIN fiber.

The random structures of different types of fs-inscribed structures in multi-mode GRIN fiber (Figure 1) were used in a Raman fiber laser for the enhancement of random distributed feedback in the half-open cavity. The laser scheme that is shown in Figure 4 is a GRIN fiber cavity directly pumped by 3 multi-mode laser diodes (LDs) with total coupled power of up to  $\sim 180$  W at 940 nm after their combination by an all-fiber combiner. The pump power was fed into a 100/140  $\mu$ m GRIN fiber with a total length of  $\sim 1$  km. An input highly reflective (HR) FBG ( $R \sim 90\%$ ) inscribed in the GRIN fiber by a CW UV laser (see [8] for details) and fabricated random reflectors as the output coupler (OC) formed the laser cavity.

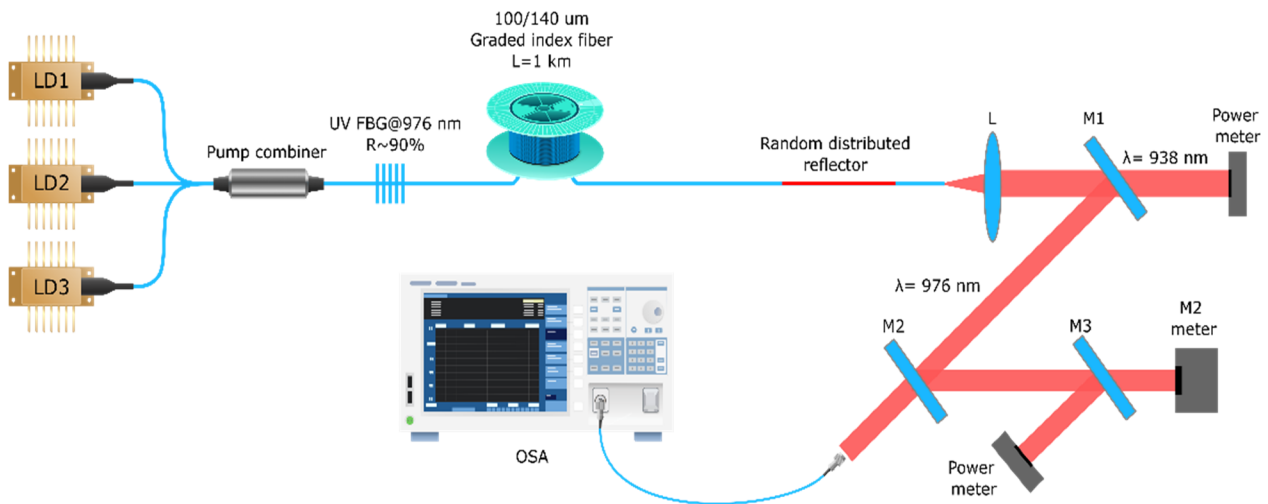


**Figure 4.** Scheme of the Raman fiber laser with a random distributed reflector.

The multi-mode Raman laser output power, spectrum and beam shape/quality were characterized by power meter (P), optical spectrum analyzer (OSA) and  $M^2$ -meter with a camera. The characterization results for the output beam generated in RFL with different random reflectors are described in the next section.

### 3. Results

#### 3.1. Multi-Mode RFL with Direct PbP-Fabricated 1D Random Structures

First, we tested a random structure of in-line (1D) point scatterers with and without a shift off the GRIN fiber axis (Figure 1a,b).

Depending of the parameters of the 1D reflector, we obtained sufficiently different characteristics. For the first sample ( $L = 120$  mm,  $\Delta L = 25$   $\mu$ m), the output power amounted to 4.7 W at  $\sim 180$  W pumping (see Figure 5), and the spectrum was concentrated near the maximum reflection of the UV-inscribed FBG. In this case, the beam quality was measured to be  $M^2 \approx 4$ , while the losses in the structure were estimated as  $\sim 50\%$ . Increasing the average distance between modified points in the longitudinal direction to  $\Delta L = 50$   $\mu$ m and shortening the entire structure length to  $L = 60$  mm (Figure 6) reduced the losses to 25–30%, improved the beam quality and increased the output power as a result. Thus, in the last configuration of the laser, power of 5.5 W was achieved at maximum pumping in spite of the higher Raman threshold ( $\sim 160$  W), with an output beam quality as good as  $M^2 \approx 2.4$ , indicating the predominant generation of fundamental mode  $LP_{01}$ .

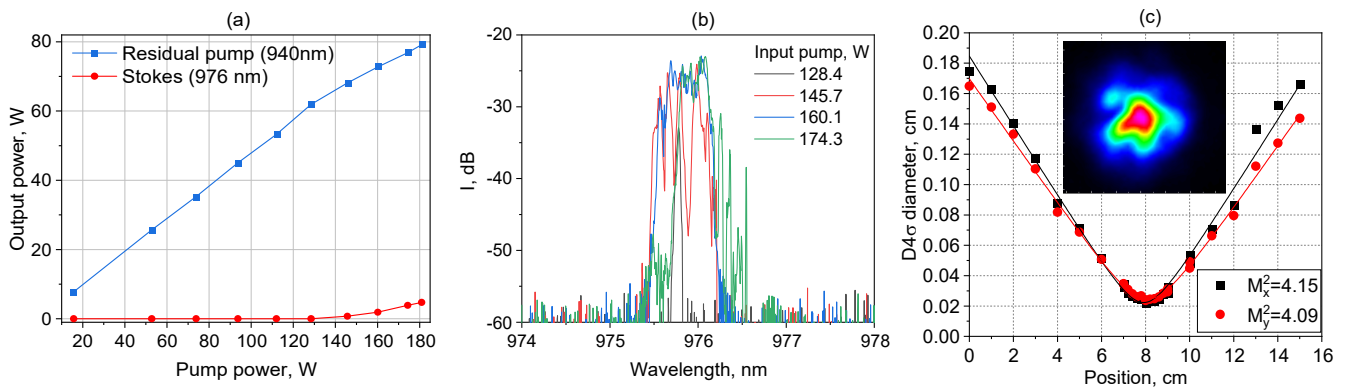


**Figure 5.** Output Stokes power together with a residual pump (a), spectra at different input pump powers (b) and output beam quality and intensity profile (color corresponds to intensity) in the waist shown in the inset, (c) of the MM RFL with an OC in-line random reflector ( $L = 120$  mm,  $\Delta L = 25$   $\mu$ m).

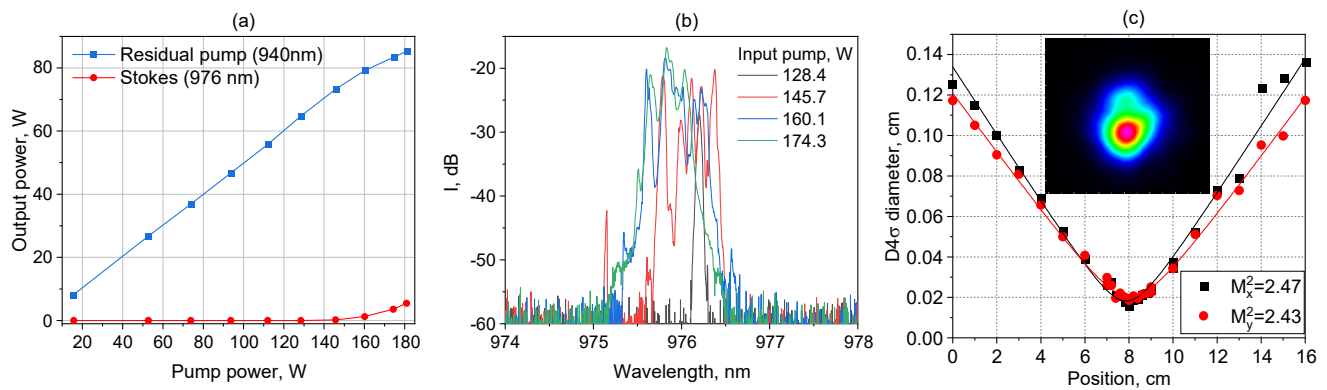


**Figure 6.** Output Stokes power together with a residual pump (a), spectra at different input pump powers (b) and output beam quality and intensity profile (color corresponds to intensity) in the waist shown in the inset (c) of the MM RFL with an OC in-line random reflector ( $L = 60 \text{ mm}$ ,  $\Delta L = 50 \text{ }\mu\text{m}$ ).

As a next step, we studied the reflectors with a relative shift in the transverse direction of  $\Delta y \sim 3 \text{ }\mu\text{m}$  as compared with the previous ones (off the fiber axis, as we supposed). It should be noted that it was difficult to say the exact relative position of the 1D random structure against the axis as the fs-inscribed scattering points had ellipsoid shapes with  $\sim 1 \times 10 \text{ }\mu\text{m}$  dimensions in the  $x$ - $y$  axes, respectively; see [4,14] for more details.

Figure 7 shows the results obtained with two successive random reflectors inscribed with a relative vertical shift  $\Delta y \sim 3 \text{ }\mu\text{m}$ , the average distance between the adjacent modification points  $\Delta L = 25 \text{ }\mu\text{m}$  and the length of each reflector  $L = 120 \text{ mm}$  (with a  $2 \times 120 \text{ mm}$  total length to lower the generation threshold). The threshold pump power in this configuration was  $\sim 140 \text{ W}$ , output power was  $3.3 \text{ W}$  at  $174 \text{ W}$  pumping, while the beam quality was  $M^2 \approx 5.4$ . In this case, the transverse intensity profile consisted of two maxima (indicating predominant  $LP_{11}$ -mode generation). The spectrum with this random output reflector was broader and exhibited stronger irregularities that were also a sign of higher-order mode generation. At the same time, the losses of the random structure were estimated to be high enough, amounting to 70–80%, which explains the lower output power in this case. Nevertheless, the main result here is that the off-axis shifted 1D random reflector allows for the selection of  $LP_{11}$  transverse mode.

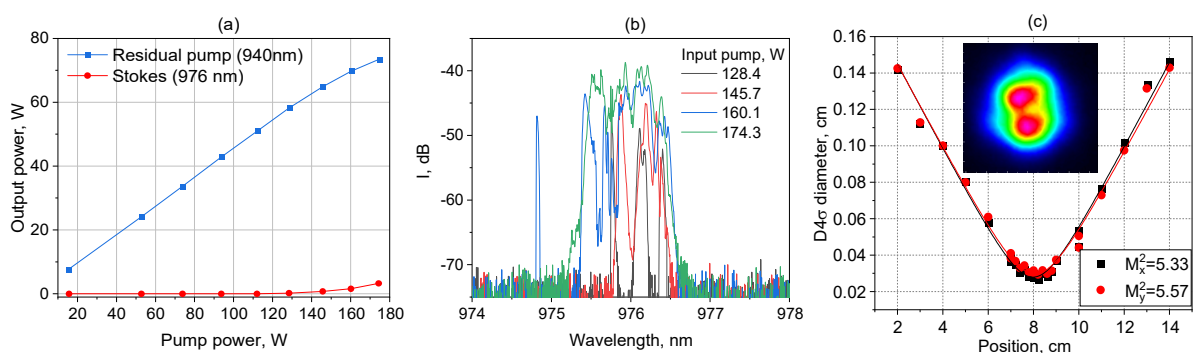


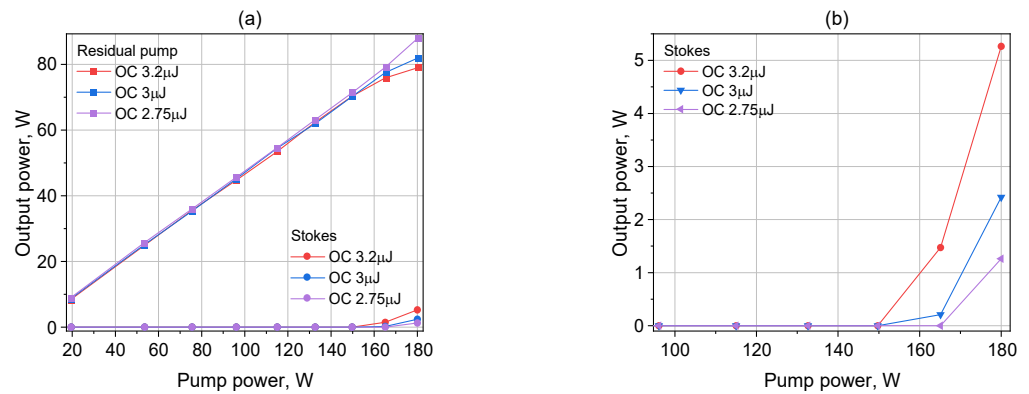
**Figure 7.** Output Stokes power together with a residual pump (a), spectra at different input pump powers (b) and output beam quality and intensity profile (color corresponds to intensity) in the waist shown in the inset (c) of the MM RFL with an OC in-line random reflector ( $L = 2 \times 120 \text{ mm}$ ,  $\Delta L = 25 \text{ }\mu\text{m}$ ) with a relative shift  $\Delta y \sim 3 \text{ }\mu\text{m}$ .

### 3.2. Multi-Mode RFL with SLM-Fabricated 3D Random Structures

In another series of experiments with multi-mode RFLs, three types of 3D random reflectors fabricated in the GRIN fiber under different conditions of SLM-assisted writing with fs pulses were used as the OC random reflectors. Three different energy levels of femtosecond pulses near optimal values ( $2.75, 3$  and  $3.2 \text{ }\mu\text{J}$ ) were selected, at which, the

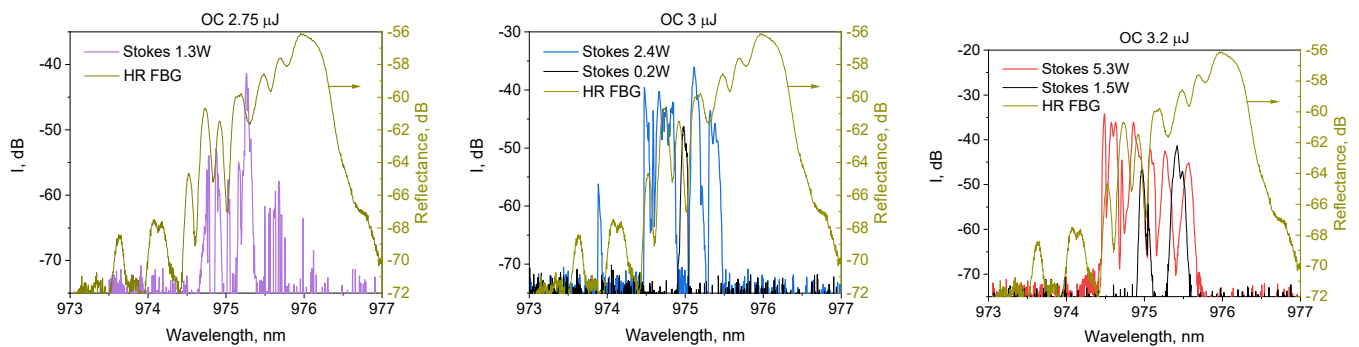
photo-modification of samples was performed. Different pulse energies during writing led to different reflection coefficients and losses of output random reflectors, and a significant difference in the output characteristics of the Raman laser was expected.

Figure 8 shows the output powers of the residual pump at 940 nm (a) and the generated Stokes wave power at 976 nm as a function of the input pump power. As expected, the maximum efficiency of Raman conversion into the Stokes wave occurred in the case of an OC random reflector written with the highest energy of fs pulses (3.2  $\mu$ J), while the Stokes generation threshold was  $\sim$ 160 W and the output Stokes power reached 5.3 W at 180 W pump power.



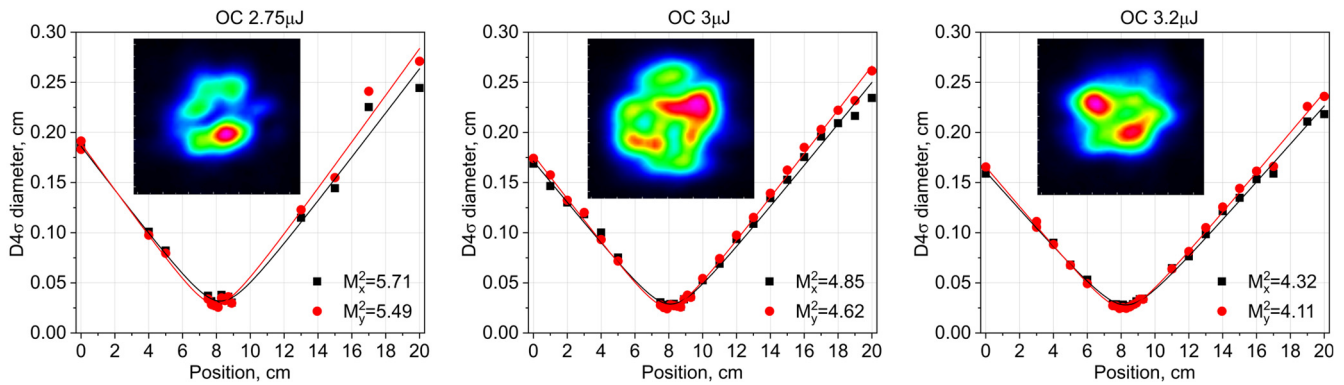
**Figure 8.** (a) Output power of laser with different samples of 3D random distributed reflectors (OC). (b) Generated Stokes power shown in larger scale.

Figure 9 shows the measured Stokes generation spectra in the schemes with different random reflectors at different Stokes power levels. It is also interesting to compare the obtained data with the reflection spectrum of an HR FBG, the maximum of which corresponded to the reflection wavelength of the fundamental mode, while the peaks located to the left of the maximum corresponded to the FBG reflection resonances of higher-order transverse modes of the GRIN fiber. Figure 9 shows that the Raman generation occurred on the short-wavelength slope of the FBG, i.e., high-order transverse modes were excited. However, for reflectors written by high-energy pulses, additional excitation with a lower-order mode occurred, i.e., it can be assumed that the reflection maximum of fs-modified rings shifted closer to the center of the fiber core. It is noteworthy that in a laser with a specific type of random reflector, with an increase in the pump power, the beam quality degraded due to the excitation of higher-order modes, as can be seen from the presented spectra. The beam quality parameter ( $M^2$ ) measurements shown in Figure 10 agree with the generation spectra analysis. Thus, when using reflectors with photo-modification pulse energies of 2.75, 3 and 3.2  $\mu$ J, the  $M^2$  parameter was consistently improved to 5.6, 4.7 and 4.2, respectively.



**Figure 9.** Output laser spectra in comparison with HR FBG reflectance spectra for different 3D random reflectors.





**Figure 10.** Measured beam quality parameter  $M^2$  for lasers with different random reflectors at maximum RFL power (from left to right): 2.75, 3, 3.2  $\mu\text{J}$ . Inset: beam intensity (marked by different colors) profile in the waist.

Figure 11 shows the output beam intensity profile for the strongest OC reflector (3.2  $\mu\text{J}$ ) captured from the plane of the fiber end face. Suppression of the fundamental mode and formation of a ring optical structure were visible, which, however, were not stable. It should be noted that the generated highly multi-mode beams in this scheme had sufficiently different shapes on the end face of the GRIN fiber near the output 3D random reflector (see Figure 11) and in the waist of the focused beam (see Figure 10). So, this fact should be considered during the analysis of the highly multi-mode beam shapes, in contrast to the beams with predominant content of a single mode (like  $\text{LP}_{01}$  or  $\text{LP}_{11}$  in Figures 6 and 7), for which the beam shape remained almost unchanged.

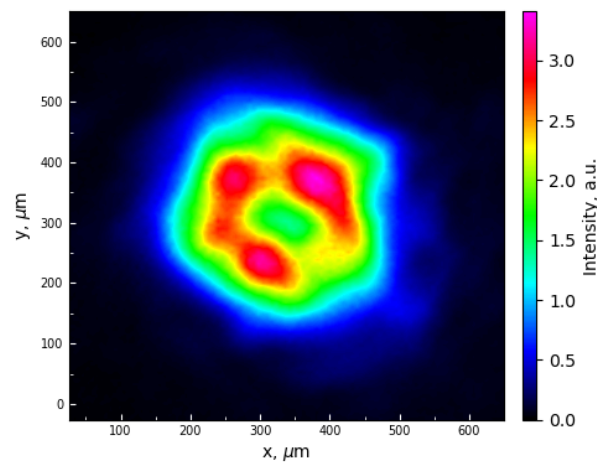


**Figure 11.** Beam intensity profile at 5.3 W output power captured in the plane of the fiber end face (OC 3.2  $\mu\text{J}$ ).

#### 4. Discussion and Conclusions

Thus, a single-stage Raman laser based on multi-mode GRIN fiber with random backscattering structures artificially induced by fs laser pulses, enhancing feedback either for the fundamental mode or higher-order modes, has been demonstrated.

It was shown that the artificial structures greatly reduced the threshold pumping (to 140–160 W) for random Raman lasing in multi-mode GRIN fiber, as compared with the random RFL scheme based on natural Rayleigh backscattering [12]. At the same time, relatively high losses in the artificial reflector (30–70%) significantly limited the efficiency of the conversion of highly multi-mode ( $M^2 \sim 34$ ) LD pump radiation (940 nm) into a Stokes beam (976 nm) with the desired transverse mode composition. Another problem is related to rather low long-term stability due to heating, although the results were usually repeated every time the laser is turned on, at least at the initial stage of laser operation.

For the 1D random reflector fs-inscribed along the GRIN fiber axis by the point-by-point technique with parameters ( $L = 60$  mm,  $\Delta L = 50$   $\mu\text{m}$ ), the Stokes radiation with beam quality improved to  $M^2 \sim 2.4$ , indicating that predominant content of the fundamental mode ( $\text{LP}_{01}$ ) was generated with output power of 5.5 W at  $\sim 180$  W pumping. It has been shown that it is possible to select higher-order  $\text{LP}_{11}$  mode when using a 1D random reflector shifted off the fiber axis in the transverse direction ( $\Delta y \sim 3$   $\mu\text{m}$  in the experiment). In this case, a typical beam with two maxima and a  $\sim 2$  times-increased beam quality parameter  $M^2$  was generated, demonstrating the possibility of such higher-order mode selection.

For the generation of more complicated transverse mode compositions in the scheme of a multi-mode LD-pumped GRIN fiber random Raman laser, we have presented a new fs laser writing technique assisted by a phase-only SLM. This writing technique provides an opportunity to move a focal spot inside static fiber, which allows for the inscription of various reflective structures with complex geometries. We optimized inscription parameters such as pulse energy, SLM frame rate and the overall length and distance of structures along the fiber by using line-by-line modification in the chosen fiber cross-section and random distances between the modified areas along the fiber, being initially optimized in a single-mode fiber. With optimal parameters, the inscription of 3D ring-shaped random structures in the 100/140  $\mu\text{m}$  GRIN multi-mode fiber was demonstrated, which allowed for the achievement of Rayleigh backscattering enhancement of up to +66 dB/mm. Such random structures with parameters ( $L = 2$  mm,  $\Delta L = 5$   $\mu\text{m}$ ) SLM-inscribed in GRIN fiber were used as random output couplers of the Raman laser cavity. The random Raman laser generated a ring-shaped output Stokes beam (with  $M^2 \sim 5$ ) out of the multi-mode fiber with relatively low pumping threshold ( $\sim 160$  W), whereas the output Stokes power amounted to 5.3 W at 180 W pumping. It should be noted that the output characteristics of the random RFL generating a ring-shape beam were close to those obtained for the RFL with 1D in-line random structures, which was in correspondence with their similar integral backscattering/loss coefficients. Let us also mention that the proposed method also allowed for the inscription of arbitrary-shape structures in multi-mode fibers to form a half-open cavity, with an artificial random reflector allowing for the selection of various transverse modes and their compositions at a relatively low generation threshold. This is especially attractive after the recent demonstration of an LD-pumped random Raman fiber laser with natural Rayleigh backscattering feedback in a multi-mode GRIN fiber of a 100  $\mu\text{m}$  core [20]. It demonstrated the high output power (0.65 kW) of the Stokes wave (1018 nm) above the relatively high threshold ( $\sim 1$  kW), which was possible to overcome due to the spectral combination of multiple LDs in the 950–990 nm spectral range.

In addition, since a random reflector in the general case is not a spectrally selective element and has weak dependence of the reflection coefficient on the wavelength, such types of Raman lasers with tunable HR FBG can be used as tunable or wavelength agile laser sources in a wide wavelength range in corresponding practical applications.

**Author Contributions:** Conceptualization, S.A.B., A.G.K. and A.V.D.; methodology, A.Y.K., D.S.K. and A.G.K.; validation, Z.E.M., A.A.R. and I.N.N.; investigation, A.G.K., A.V.D., Z.E.M. and P.A.E.; writing—original draft preparation, A.G.K., Z.E.M. and A.V.D.; writing—review and editing, S.A.B.; supervision and funding acquisition, S.A.B. All authors have read and agreed to the published version of the manuscript.

**Funding:** This research was funded by the RUSSIAN SCIENCE FOUNDATION, grant number 21-72-30024.

**Data Availability Statement:** Data available upon request.

**Acknowledgments:** The work was carried out using the equipment of the Center for Collective Use “Spectroscopy and Optics” of the IAE SB RAS. We acknowledge the help of A. Wolf during the initial stage of the work.

**Conflicts of Interest:** The authors declare no conflicts of interest.

## References

1. Richardson, D.J.; Fini, J.M.; Nelson, L. Space-division multiplexing in optical fibres. *Nat. Photonics* **2013**, *7*, 354–362. [[CrossRef](#)]
2. Jaregui, C.; Limpert, J.; Tünnermann, A. High-power fibre lasers. *Nat. Photonics* **2013**, *7*, 861–867. [[CrossRef](#)]
3. Richardson, D.J.; Nilsson, J.; Clarkson, W.A. High power fiber lasers: Current status and future perspectives. *JOSA B* **2010**, *27*, B63–B92. [[CrossRef](#)]
4. Babin, S.A.; Zlobina, E.A.; Kablukov, S.I. Multimode Fiber Raman Lasers Directly Pumped by Laser Diodes. *IEEE J. Sel. Top. Quantum Electron.* **2018**, *24*, 1–10. [[CrossRef](#)]
5. Glick, Y.; Shamir, Y.; Sintov, Y.; Goldring, S.; Pearl, S. Brightness enhancement with Raman fiber lasers and amplifiers using multi-mode or multi-clad fibers. *Opt. Fiber Technol.* **2019**, *52*, 101955. [[CrossRef](#)]
6. Supradeepa, V.R.; Feng, Y.; Nicholson, J.W. Raman fiber lasers. *J. Opt.* **2017**, *19*, 023001. [[CrossRef](#)]
7. Terry, N.B.; Alley, T.G.; Russell, T.H. An explanation of SRS beam cleanup in graded-index fibers and the absence of SRS beam cleanup in step-index fibers. *Opt. Express* **2007**, *15*, 17509. [[CrossRef](#)] [[PubMed](#)]
8. Kuznetsov, A.G.; Kablukov, S.I.; Podivilov, E.V.; Babin, S.A. Brightness enhancement and beam profiles in an LD-pumped graded-index fiber Raman laser. *OSA Contin.* **2021**, *4*, 1034–1040. [[CrossRef](#)]
9. Evmenova, E.A.; Kuznetsov, A.G.; Nemov, I.N.; Wolf, A.A.; Dostovalov, A.V.; Kablukov, S.I.; Babin, S.A. 2nd-order random lasing in a multimode diode-pumped graded-index fiber. *Sci. Rep.* **2018**, *8*, 17495. [[CrossRef](#)] [[PubMed](#)]
10. Kuznetsov, A.G.; Nemov, I.N.; Wolf, A.A.; Evmenova, E.A.; Kablukov, S.I.; Babin, S.A. Cascaded generation in multimode diode-pumped graded-index fiber Raman lasers. *Photonics* **2021**, *8*, 447. [[CrossRef](#)]
11. Babin, S.A.; Dontsova, E.I.; Kablukov, S.I. Random fiber laser directly pumped by a high-power laser diode. *Opt. Lett.* **2013**, *38*, 3301–3303. [[CrossRef](#)] [[PubMed](#)]
12. Chen, Y.; Fan, C.; Yao, T.; Xiao, H.; Leng, J.; Zhou, P.; Nemov, I.N.; Kuznetsov, A.G.; Babin, S.A. Brightness enhancement in random Raman fiber laser based on a graded-index fiber with high-power multimode pumping. *Opt. Lett.* **2021**, *46*, 1185–1188. [[CrossRef](#)] [[PubMed](#)]
13. Turitsyn, S.K.; Babin, S.A.; Churkin, D.V.; Vatik, I.D.; Nikulin, M.; Podivilov, E.V. Random distributed feedback fibre lasers. *Phys. Rep.* **2014**, *542*, 133–193. [[CrossRef](#)]
14. Dostovalov, A.; Wolf, A.; Munkueva, Z.; Skvortsov, M.; Abdullina, S.; Kuznetsov, A.; Babin, S. Continuous and discrete-point Rayleigh reflectors inscribed by femtosecond pulses in singlemode and multimode fibers. *Opt. Laser Technol.* **2023**, *167*, 109692. [[CrossRef](#)]
15. Westbrook, P.S.; Feder, K.S.; Kremp, T.; Monberg, E.M.; Wu, H.; Zhu, B.; Huang, L.; Simoff, D.A.; Shenk, S.; Handerek, V.A.; et al. Enhanced Optical Fiber for Distributed Acoustic Sensing beyond the Limits of Rayleigh Backscattering. *iScience* **2020**, *23*, 101137. [[CrossRef](#)] [[PubMed](#)]
16. Fuertes, V.; Grégoire, N.; Labranche, P.; Gagnon, S.; Rivera VA, G.; LaRochelle, S.; Messaddeq, Y. Tunable Rayleigh scattering in low-loss Sr-based nanoparticle-doped optical fibers: Controlling nanoparticle features throughout preform and fiber fabrication. *J. Alloys Compd.* **2023**, *940*, 168928. [[CrossRef](#)]
17. Wang, M.; Zhao, K.; Wu, J.; Li, Y.; Yang, Y.; Huang, S.; Zhao, J.; Tweedle, T.; Carpenter, D.; Zheng, G.; et al. Femtosecond laser fabrication of nanograting-based distributed fiber sensors for extreme environmental applications. *Int. J. Extrem. Manuf.* **2021**, *3*, 025401. [[CrossRef](#)]
18. Salter, P.S.; Booth, M.J. Adaptive optics in laser processing. *Light Sci. Appl.* **2019**, *8*, 110. [[CrossRef](#)] [[PubMed](#)]
19. Dostovalov, A.; Kokhanovskiy, A.; Golikov, E.; Revyakin, A.; Munkueva, Z.; Kharenko, D.; Babin, S. Fiber Bragg grating inscription assisted by a spatial light modulator. *Opt. Lett.* **2024**, *49*, 1077–1080. [[CrossRef](#)] [[PubMed](#)]
20. Hao, X.; Fan, C.; Li, Y.; Pan, Z.; Leng, J.; Yao, T.; Lei, B.; Zhou, P. Brightness enhancement on random-distributed-feedback Raman fiber lasers pumped by multimode diodes. In *High Power Laser Science and Engineering*; Cambridge University Press: Cambridge, UK, 2024. [[CrossRef](#)]

**Disclaimer/Publisher’s Note:** The statements, opinions and data contained in all publications are solely those of the individual author(s) and contributor(s) and not of MDPI and/or the editor(s). MDPI and/or the editor(s) disclaim responsibility for any injury to people or property resulting from any ideas, methods, instructions or products referred to in the content.